# Factors affecting physical and physicochemical properties of NR/SBR rubber blends: I) Effect of blending ratio on the stress-strain characteristics for pure and carbon blacks filled composites

H.H. Hassan, S.S. Abdel-Aziz, A.S. Abdel-Rahman* and M.H. Soleiman

Physics Department, Faculty of Science, Cairo University, Giza, Egypt
*asabry@sci.cu.educ.com

**Abstract:** Blends of Natural Rubber/Styrene Butadiene Rubber (NR/SBR) loaded with different ratios of N220:N774 carbon black fillers were prepared. The mechanical properties of pure blends and those loaded with different ratios of carbon black were investigated. The (50NR/50SBR), 40N220/(50NR/50SBR) and 60N774/(50NR/50SBR) blends were found to exhibit the highest values of tensile strength and elongation at break. The theoretical Mooney-Rivlin model was applied to NR/SBR where it supports the result of stress-strain characteristics. (50NR/50SBR) blends loaded with mixed ratios of N220 and N774 blacks were also prepared. The stress-strain study did not show any significant change due to the order of addition of carbon black. The values of shore hardness (A) for all samples were measured and showed a marked increase by increasing the black content. The relation between the volume concentration and the filler concentration (phr) for each carbon types is found to follow power laws.

[Hassan HH, Abdel-Aziz SS, Abdel-Rahman AS and Soleiman MH. **Factors affecting physical and physicochemical properties of NR/SBR rubber blends: I) Effect of blending ratio on the stress-strain characteristics for pure and carbon blacks filled composites.** *Nat Sci* 2015;13(8):117-126]. (ISSN: 1545-0740). http://www.sciencepub.net/nature. 19

**Keywords:** Carbon black, NR rubber, SBR rubber, stress, strain, order of addition, power law

## 1. Introduction

Blending two or more polymers to produce new materials with mixed properties has been extensively developed in several industries [1,2]. Natural rubber (NR) crystallizes under stretching, so that it resists deformation and enhances its strength while many synthetic rubbers such as styrene butadiene rubber (SBR)-1502 does not crystallize. Mixtures of NR and SBR are quite often used in order to get desired technological properties [2-4].

Carbon black is widely used as a filler to enhance the performance of rubbers and other polymeric materials [5]. The reinforcement of elastomers by particulate fillers has been deeply studied in numerous investigations [6,7], and it is generally accepted that this phenomenon is, to a large extent, dependant on the physical interactions between the filler and the rubber matrix. The structure, surface characteristics and especially particle size of the fillers are the main factors that determine their reinforcing effects of composites [8].

The classical kinetic theory of rubber elasticity originally developed by Wall [9], Flory [10] and James & Guth [11] attributed the high elasticity of a cross-liked rubber to the change of the conformational entropy of long flexible molecular chains.

Mooney and Rivlin [12,13] theoretical approaches can describe the filler free blends according to relation plots of true stress ($\sigma$) and elongation ($\lambda$) in Gaussian region, while Guth, Simha and Gold [14-16] introduce a relation for filler volume concentration applied in case of carbon loaded samples.

In the present work, the mechanical properties of pure NR/SBR blends and those loaded with different ratios of two types of carbon blacks were studied. Mixed ratios of carbon black were also added to the rubber optimum blend in order to show the optimum values of mechanical properties, based on the theoretical models. The stress-strain curves were fitted to theoretical equations to discuss the density of cross-linking and its dependence on the blend ratio.

## 2. Experimental

### 2.1. Materials

The samples under investigation were divided into three main groups:

2.1.1) Carbon free samples, they are denoted by NS and refer to the rubber blend of NR and SBR-1502 with different ratios. The compounding formulations (recipes) of composites are listed in Table (1).

2.1.2) The optimum sample (NS55) was loaded with (N220) and (N774) black to form NS55N2 and NS55N7 samples, respectively. Each of them was studies with concentration increment of 10 phr of carbon black. The terms N2 and N7 refer to N220 and N774 blacks, respectively, and the carbon concentration in phr appears at the end of blend name

(L10, L20, …, L100) as shown in Table (2) and Table (3).

2.1.3) The order of addition of carbon to NS55 blend was presented in Tables (4) and (5). The notation N2N7 and N7N2 refer to the pure blend NS55 loaded with N220 carbon first and then N774 and vice versa, respectively. For example NS55N2N7L14 refers to N220 concentration is 10 phr and N774 concentration is 40 phr.

**2.2 Samples preparation**

All rubber compounds were mixed according to the ASTM D 3182 [17] standard by using a two-roll mill of 300 mm length, 150 mm diameter, speed of slow roll 18 rpm and gear ratio 1.4. The compounded rubbers were molded into dumbbell-shaped specimens of 2 mm thick, 7 mm width, and 100 mm length.

The vulcanization process was carried out by using an electrically heated platen press at 143±2°C and 15 MPa for 30 min.

Table 1. The compounding recipe of the NS blends

| Ingredients(phr)* | NS01 | NS19 | NS28 | NS37 | NS46 | NS55 | NS64 | NS73 | NS82 | NS91 | NS10 |
|---|---|---|---|---|---|---|---|---|---|---|---|
| NR | 0 | 10 | 20 | 30 | 40 | 50 | 60 | 70 | 80 | 90 | 100 |
| SBR-1502 | 100 | 90 | 80 | 70 | 60 | 50 | 40 | 30 | 20 | 10 | 0 |
| Stearic acid | 2 | 2 | 2 | 2 | 2 | 2 | 2 | 2 | 2 | 2 | 2 |
| ZnO | 5 | 5 | 5 | 5 | 5 | 5 | 5 | 5 | 5 | 5 | 5 |
| Processing Oil | 10 | 10 | 10 | 10 | 10 | 10 | 10 | 10 | 10 | 10 | 10 |
| MBTS** | 2 | 2 | 2 | 2 | 2 | 2 | 2 | 2 | 2 | 2 | 2 |
| IPPD 4020*** | 1 | 1 | 1 | 1 | 1 | 1 | 1 | 1 | 1 | 1 | 1 |
| Sulfur | 2 | 2 | 2 | 2 | 2 | 2 | 2 | 2 | 2 | 2 | 2 |

* Part per hundred parts of rubber by weight in grams.
** MBTS methylebenzthiazyle disulfide (accelerator)
*** IPPD 4020 N-isopropyl-N'-phenyl-p-phenylene diamine (antioxidant, antiozonant and antiflex)

Table 2. The compounding recipe of the NS55N2 Samples

| Ingredients(phr) | NS55 N2L10 | NS55 N2L20 | NS55 N2L30 | NS55 N2L40 | NS55 N2L50 | NS55 N2L60 | NS55 N2L70 | NS55 N2L80 | NS55 N2L90 | NS55N2 L100 |
|---|---|---|---|---|---|---|---|---|---|---|
| NR | 50 | 50 | 50 | 50 | 50 | 50 | 50 | 50 | 50 | 50 |
| SBR-1502 | 50 | 50 | 50 | 50 | 50 | 50 | 50 | 50 | 50 | 50 |
| Stearic acid | 2 | 2 | 2 | 2 | 2 | 2 | 2 | 2 | 2 | 2 |
| ZnO | 5 | 5 | 5 | 5 | 5 | 5 | 5 | 5 | 5 | 5 |
| Processing Oil | 10 | 10 | 10 | 10 | 10 | 10 | 10 | 10 | 10 | 10 |
| N220 | 10 | 20 | 30 | 40 | 50 | 60 | 70 | 80 | 90 | 100 |
| MBTS | 2 | 2 | 2 | 2 | 2 | 2 | 2 | 2 | 2 | 2 |
| IPPD 4020 | 1 | 1 | 1 | 1 | 1 | 1 | 1 | 1 | 1 | 1 |
| Sulfur | 2 | 2 | 2 | 2 | 2 | 2 | 2 | 2 | 2 | 2 |

Table 3. The compounding recipe of the NS55N7 Samples

| Ingredients(phr) | NS55 N7L10 | NS55 N7L20 | NS55 N7L30 | NS55 N7L40 | NS55 N7L50 | NS55 N7L60 | NS55 N7L70 | NS55 N7L80 | NS55 N7L90 | NS55N7 L100 |
|---|---|---|---|---|---|---|---|---|---|---|
| NR | 50 | 50 | 50 | 50 | 50 | 50 | 50 | 50 | 50 | 50 |
| SBR-1502 | 50 | 50 | 50 | 50 | 50 | 50 | 50 | 50 | 50 | 50 |
| Stearic acid | 2 | 2 | 2 | 2 | 2 | 2 | 2 | 2 | 2 | 2 |
| ZnO | 5 | 5 | 5 | 5 | 5 | 5 | 5 | 5 | 5 | 5 |
| Processing Oil | 10 | 10 | 10 | 10 | 10 | 10 | 10 | 10 | 10 | 10 |
| N774 | 10 | 20 | 30 | 40 | 50 | 60 | 70 | 80 | 90 | 100 |
| MBTS | 2 | 2 | 2 | 2 | 2 | 2 | 2 | 2 | 2 | 2 |
| IPPD 4020 | 1 | 1 | 1 | 1 | 1 | 1 | 1 | 1 | 1 | 1 |
| Sulfur | 2 | 2 | 2 | 2 | 2 | 2 | 2 | 2 | 2 | 2 |

Table 4. The compounding recipe of the NS55N2N7 Samples

| Ingredients(phr) | NS55N2N7L14 | NS55N2N7L23 | NS55N2N7L32 | NS55N2N7L41 |
|---|---|---|---|---|
| NR | 50 | 50 | 50 | 50 |
| SBR-1502 | 50 | 50 | 50 | 50 |
| Stearic acid | 2 | 2 | 2 | 2 |
| ZnO | 5 | 5 | 5 | 5 |
| Processing Oil | 10 | 10 | 10 | 10 |
| N220 | 10 | 20 | 30 | 40 |
| N774 | 40 | 30 | 20 | 10 |
| MBTS | 2 | 2 | 2 | 2 |
| IPPD 4020 | 1 | 1 | 1 | 1 |
| Sulfur | 2 | 2 | 2 | 2 |

Table 5. The compounding recipe of the NS55N7N2 Samples

| Ingredients(phr) | NS55N7N2L14 | NS55N7N2L23 | NS55N7N2L32 | NS55N7N2L41 |
|---|---|---|---|---|
| NR | 50 | 50 | 50 | 50 |
| SBR-1502 | 50 | 50 | 50 | 50 |
| Stearic acid | 2 | 2 | 2 | 2 |
| ZnO | 5 | 5 | 5 | 5 |
| Processing Oil | 10 | 10 | 10 | 10 |
| N774 | 10 | 20 | 30 | 40 |
| N220 | 40 | 30 | 20 | 10 |
| MBTS | 2 | 2 | 2 | 2 |
| IPPD 4020 | 1 | 1 | 1 | 1 |
| Sulfur | 2 | 2 | 2 | 2 |

**2.3. Mechanical Test**

Mechanical test was carried out at room temperature by using a homemade tensile testing machine of cross head speed of 115 mm/min according to ASTM D 412-80 [18]. The true stress ($\sigma$) and true strain ($\varepsilon$) were calculated according to the formulas 1 and 3 [19, 20] respectively:

$$\sigma = \frac{F}{A_0}\lambda \quad \text{.... (1)}$$

where $F$ is the applied force, $A_0$ is the initial cross sectional area of the sample and $\lambda$ is the elongation which is;

$$\lambda = \frac{l}{l_0} \quad \text{.... (2)}$$

$$\varepsilon = \ln(\lambda) \quad \text{.... (3)}$$

where $l$ is the length of sample under stress while $l_0$ is the initial length of sample.

**2.4. Hardness Testing**

The hardness studied by NT-6510 Shore Hardness Tester for five specimen of each sample, each of them was disc of 30 mm diameter and 12 mm thick.

**3. Results and Discussion**

**3.1. NS blends**

Figure (1) shows the stress-stain curves for NS blends, which report an optimum value at the ratio 50 phr of NR and 50 phr of SBR. This result is also achieved from the values of tensile strength and elongation at break which presented in Figure (2). These results were found to be in good agreement with Ref. [21].

The modulus of elasticity, $E$ (Table (6)) shows a maximum value for NS55 blend which is in good agreement with the above obtained data.

The hardness study represents linear decrease of shore A value by negative slope of 0.17 with increasing the NR content in the blend as shown in Figure (3). This can be attributed to the nature of NR which resists mechanical deformation and enhances blend strength; while SBR increases the values of hardness of the blend quit to its 60% than the pure NR sample.

According to the previous results, the optimum strengthen blend is NS55, in which carbon black will be then introduced.

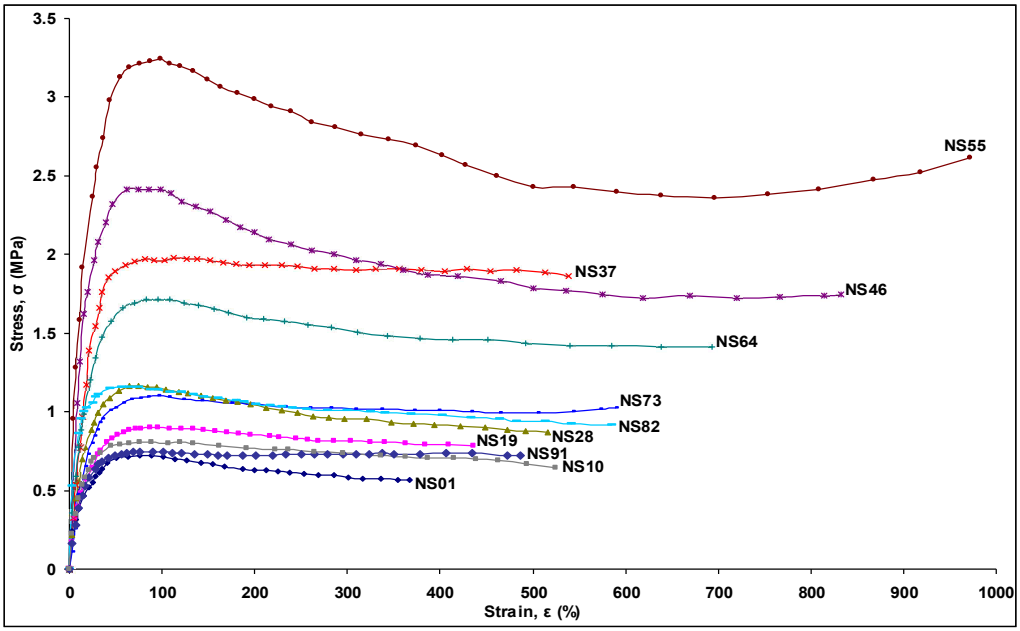


Figure 1. Stress-strain characteristics for NS blends

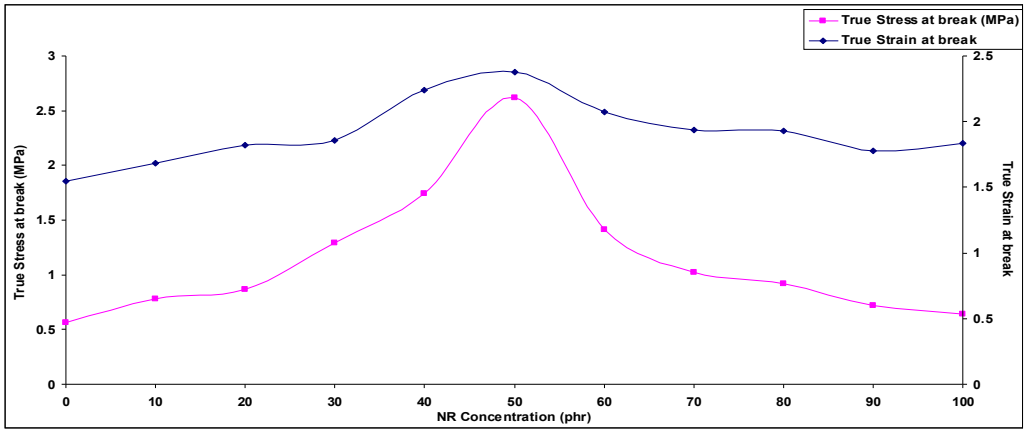


Figure 2. True stress at break and true strain at break versus NR content for NS blends

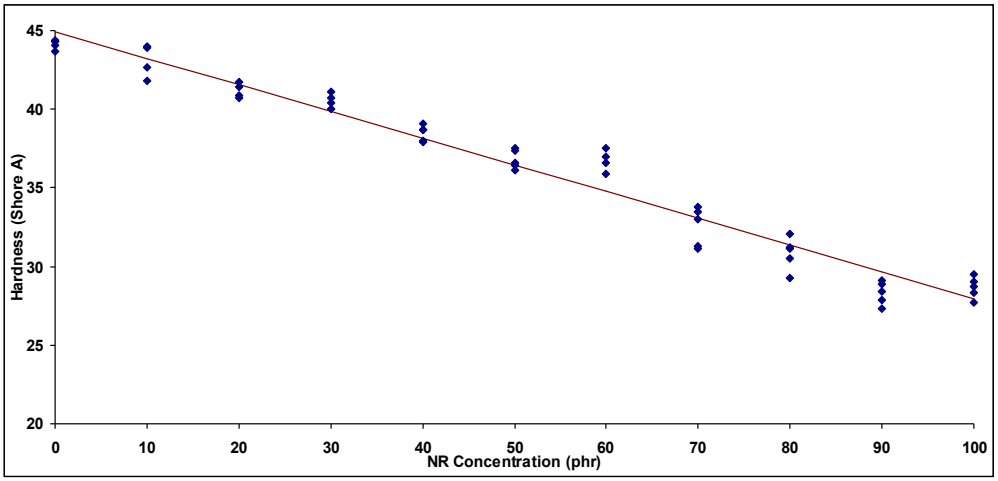


Figure 3. Hardness versus NR concentration for NS blends

Table 6. The modulus of elasticity (*E*) of the NS blends

| Sample | NS01 | NS19 | NS28 | NS37 | NS46 | NS55 | NS64 | NS73 | NS82 | NS91 | NS10 |
|---|---|---|---|---|---|---|---|---|---|---|---|
| NR (phr) | 0 | 10 | 20 | 30 | 40 | 50 | 60 | 70 | 80 | 90 | 100 |
| *E* (MPa) | 4.92 | 5.15 | 7.20 | 10.48 | 13.80 | 17.73 | 9.10 | 5.65 | 5.37 | 4.92 | 5.75 |

### 3.2. NS55N2 samples

Figure (4) shows stress-strain characteristics for NS55N2 samples. It is noticed that, the addition of carbon black results in a marked increase of tensile strength and elongation at break values. The closed inspection of the values presented in Figures (1, 4) show a jump of about ten times of true stress from 2.5 MPa to about 25 MPa. Sample NS55N2L40 exhibits the maximum values of true stress and true strain as shown in Figure (5).

Table (7) shows the modulus of elasticity (*E*) and the shore hardness A for NS55N2 samples.

It is noticed that the values of shore hardness A increase approximately by linear relation of slope 0.57 to reach about 2.5 of its initial value at 100 phr of carbon black content. The peak value of *E* at 40 phr of N220 confirms the above obtained results.

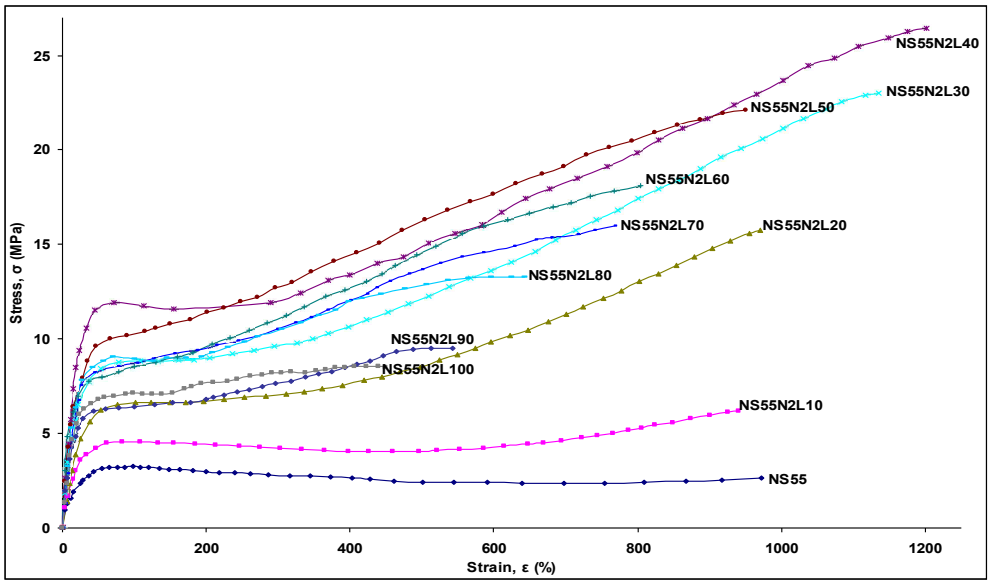


Figure 4. Stress-strain characteristics for NS55N2 blends

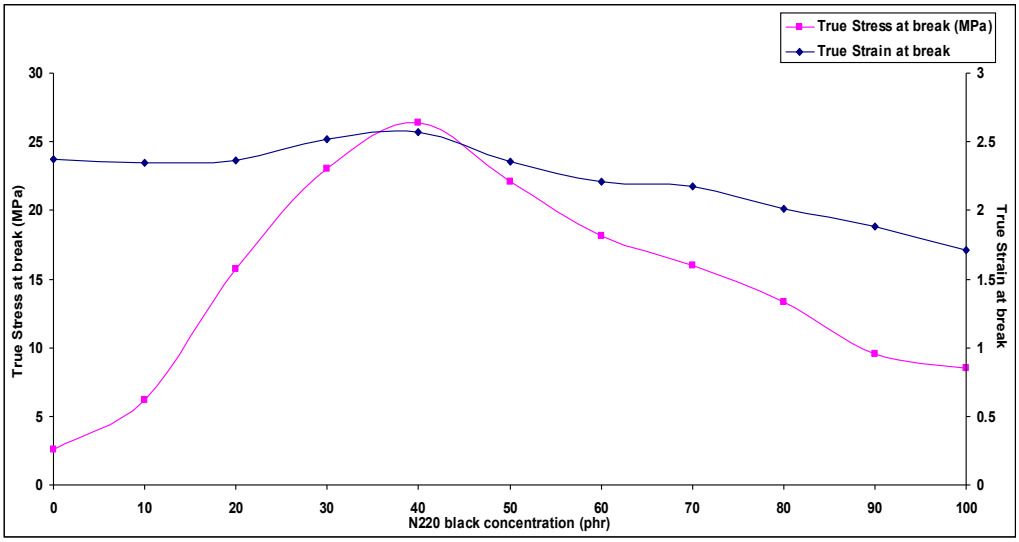


Figure 5. True stress at break and true strain at break versus N220 black concentration for NS55N2 samples

Table 7. The modulus of elasticity (*E*) and shore hardness A for NS55N2 samples

| Sample | N220 content (phr) | *E* (MPa) | Shore A |
|---|---|---|---|
| NS55 | 0 | 17.73 | 36.46 |
| NS55N2L10 | 10 | 26.23 | 42.17 |
| NS55N2L20 | 20 | 31.81 | 47.88 |
| NS55N2L30 | 30 | 48.48 | 53.60 |
| NS55N2L40 | 40 | 69.23 | 59.31 |
| NS55N2L50 | 50 | 54.89 | 65.02 |
| NS55N2L60 | 60 | 58.27 | 70.73 |
| NS55N2L70 | 70 | 52.90 | 76.45 |
| NS55N2L80 | 80 | 60.43 | 82.16 |
| NS55N2L90 | 90 | 48.78 | 87.87 |
| NS55N2L100 | 100 | 50.01 | 93.58 |

### 3.3. NS55N7 samples

Figure (6) shows the stress-strain characteristics for NS55N7 samples.

Figure (7) shows the relation between true stress at break and true strain at break versus the carbon black concentration, which indicate that the optimum value was achieved by sample NS55N7L60 and pointing slightly lower values than NS55N2 samples (Figure 4). The modulus of elasticity (*E*) and shore hardness A are shown in Table (8).

It is noticed that, hardness value grows up to nearly double for NS22N7L100 than the carbon free sample NS55, which indicates that N774 adds little strength to the pure blend. The peak value of *E* at 60 phr of N774 confirms the above obtained results.

According to the previous illustrated results, the N220 carbon reflects high strength and more hardness than N774 but they show optimum strength of blend at 40 phr and 60 phr for N220 and N774 respectively. The effect of addition of two different carbon blacks with various ratios as well as the order of addition on the physical parameters will be now studied.

Table 8. The modulus of elasticity (*E*) and shore hardness A for NS55N7 samples

| Sample | N774 content (phr) | *E* (MPa) | Shore A |
|---|---|---|---|
| NS55 | 0 | 17.73 | 36.46 |
| NS55N7L10 | 10 | 29.77 | 40.98 |
| NS55N7L20 | 20 | 33.54 | 45.50 |
| NS55N7L30 | 30 | 51.30 | 50.02 |
| NS55N7L40 | 40 | 41.10 | 54.54 |
| NS55N7L50 | 50 | 36.78 | 59.07 |
| NS55N7L60 | 60 | 52.06 | 63.59 |
| NS55N7L70 | 70 | 47.55 | 68.11 |
| NS55N7L80 | 80 | 25.91 | 72.63 |
| NS55N7L90 | 90 | 37.82 | 77.15 |
| NS55N7L100 | 100 | 23.89 | 81.67 |

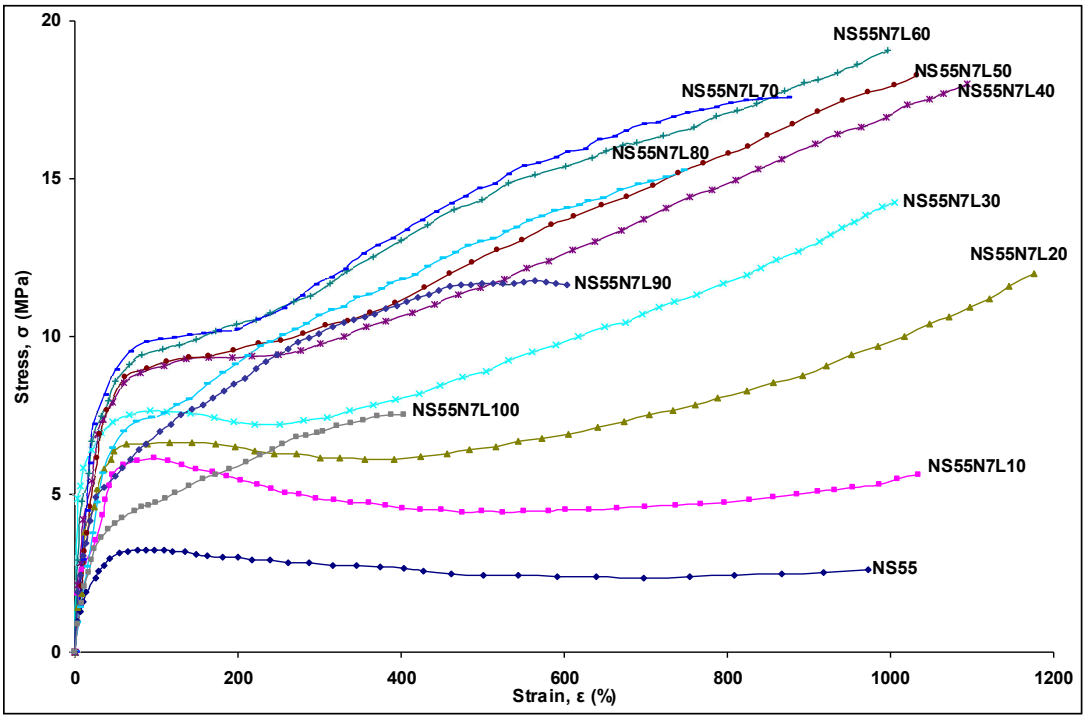


Figure 6. Stress-strain characteristics for NS55N7 blends

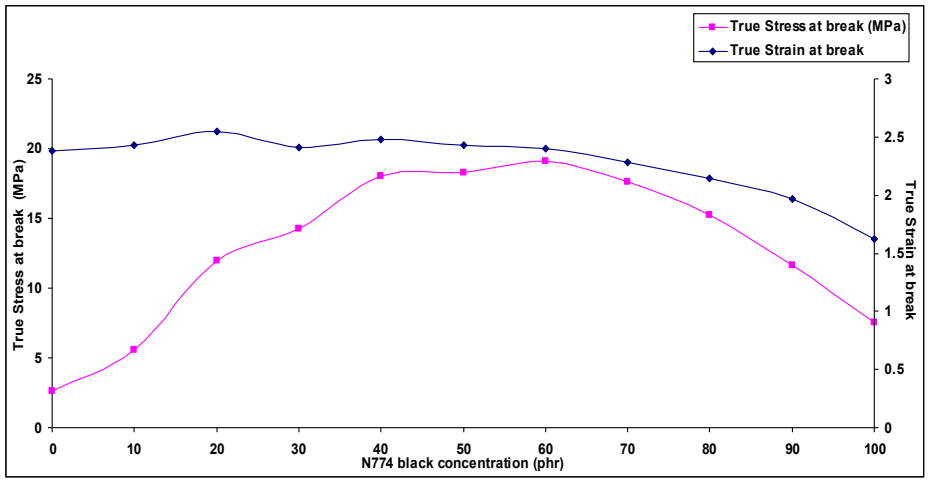


Figure 7. True stress at break and true strain at break versus N774 concentration for NS55N7 samples

### 3.4. NS55N2N7 and NS55N7N2 samples

True stress at break, true stain at break, modulus of elasticity ($E$) and shore hardness A are tabulated in Tables (9) and (10) for NS55N2N7 and NS55N7N2 samples, respectively.

It is noticed that, the order of addition of carbons rarely affects the strength of the samples; also the modulus of elasticity ($E$) and hardness test support this point where the slope of fitting lines for shore hardness in NS55N2N7 and NS55N7N2 are 0.135 and 0.120, respectively, and they almost too tight.

Table 9. The true stress at break, true stain at break, modulus of elasticity ($E$) and shore hardness A for NS55N2N7 samples

| Sample | True stress at break (MPa) | True strain at break | $E$ (MPa) | Shore A |
|---|---|---|---|---|
| NS55N7L50 | 18.27 | 2.43 | 36.78 | 60.35 |
| NS55N2N7L14 | 18.91 | 2.40 | 51.60 | 61.70 |
| NS55N2N7L23 | 19.99 | 2.39 | 50.20 | 63.06 |
| NS55N2N7L32 | 21.26 | 2.39 | 67.97 | 64.41 |
| NS55N2N7L41 | 21.23 | 2.41 | 57.85 | 65.76 |
| NS55N2L50 | 22.10 | 2.36 | 54.89 | 67.12 |

Table 10. The true stress at break, true stain at break, modulus of elasticity ($E$) and shore hardness A for NS55N7N2 samples

| Sample | True stress at break (MPa) | True strain at break | $E$ (MPa) | Shore A |
|---|---|---|---|---|
| NS55N2L50 | 22.10 | 2.36 | 54.89 | 67.12 |
| NS55N7N2L14 | 21.63 | 2.38 | 53.51 | 65.44 |
| NS55N7N2L23 | 20.50 | 2.39 | 63.61 | 64.24 |
| NS55N7N2L32 | 18.53 | 2.38 | 45.28 | 63.04 |
| NS55N7N2L41 | 18.87 | 2.39 | 69.34 | 61.84 |
| NS55N7L50 | 18.27 | 2.43 | 63.78 | 60.64 |

### 3.5. Data modeling

Mooney and Rivlin [12, 13] statistical polymer model of Gaussian [19] articulated segmental chain with links lead to an equation which may be written as:

$$\sigma(\lambda) = C_1\left(\lambda^2 - \frac{1}{\lambda}\right) + C_2\left(\lambda - \frac{1}{\lambda^2}\right) \quad \text{…. (4)}$$

This relation between true stress ($\sigma$) and elongation ($\lambda=\varepsilon+1$) should be applied to Gaussian region of $\sigma$-$\lambda$ plot, and this region could be found by rewrite equation 4 as:

$$\sigma \Big/ \left(\lambda - \frac{1}{\lambda^2}\right) = C_1\lambda + C_2 \quad \text{…. (5)}$$

Plotting the relation between $\sigma \Big/ \left(\lambda - \frac{1}{\lambda^2}\right)$ and $\lambda$ results in a straight line of slope $C_1$.

$$C_1 = NkT \quad \text{…. (6)}$$

where $N$ is the number of effective plastic chains per unit volume; $k$ is Boltzmann's constant, $T$ the absolute temperature. Where Figure (8) shows relation (5) for three samples namely NS01, NS55, and NS10. The dashed lines represent the straight line fitting in Gaussian region in range about 1.5~2.5 of elongation.

By using the above model, the constants $C_1$ and $C_2$ were calculated and listed in Table (11), beside the correlation coefficient $R^2$ value for the fitting.

Figure (9) shows strong correlation between the true strain at break and the shear modulus $C_1$ for NS samples. It is seems that the NR concentrations for the prepared samples are classified into two ranges. The first sub-range is for samples NS01-

NS55 gives correlation coefficient 0.936 using least square method. The phr concentrations of the samples NS55-NS10 are in the second sub-range and show a strong correlation with a correlation coefficient 0.784.

However, the shear modulus is determined from fitting of the Gaussian region of stress-strain curve for each sample ($\lambda$=1.2~3) the correlations in Figure (9) give information about the strains at break.

Guth, Simha and Gold [14-16] introduce relation between the shear modulus $E_f$ for carbon loaded rubber and the volume concentration of filler $C$ as:

$$E_f = E_0\left(1+0.67fC+1.62f^2C^2\right) \quad \ldots. (7)$$

where $E_f$ equals $C_1$ in case of filled rubber and $E_0$ is that of filler free rubber. The asymmetry coefficient or shape factor ($f$) is used to fit the theoretical and experimental data and its typical value was found to be 6 [19].

Volume concentration can be achieved for each sample by filler phr value, the volume density of vulcanized rubber and the known density of carbon filler.

$$\begin{aligned} &phr\ of\ [rubber+filler] \rightarrow mass\ of\ sample \\ &phr\ of\ [filler] \rightarrow mass\ of\ filler \end{aligned} \quad \ldots. (8)$$

$$volume\ concentration\ of\ filler\ (C) = \frac{volume\ of\ filler}{total\ volume\ of\ the\ sample} \quad \ldots. (9)$$

$$volume\ of\ filler\ inside\ the\ sample = \frac{mass\ of\ filler}{density\ of\ the\ filler} \quad \ldots. (10)$$

Figures (10, 11) show the factor $fC$ versus N220 phr concentration in NS55N2 samples and N774 in NS55N7 samples, respectively. $fC$ represents the results of equation (7), $fC'$ represents the calculated volume concentration multiplied by best value of $f$ which fit the two curves.

It is found that, the $fC$ factor depends monotonically on the filler phr concentration as power low with power index 0.6413 for NS55N2 and 0.7268 for NS55N7.

The calculated volume concentration $fC'$ shows a consistent behavior to the $fC$ obtained from equation (7).

Table (12) show the power low, its fit correlation $R^2$ value and $f$ value for both NS55N2 and NS55N7 samples.

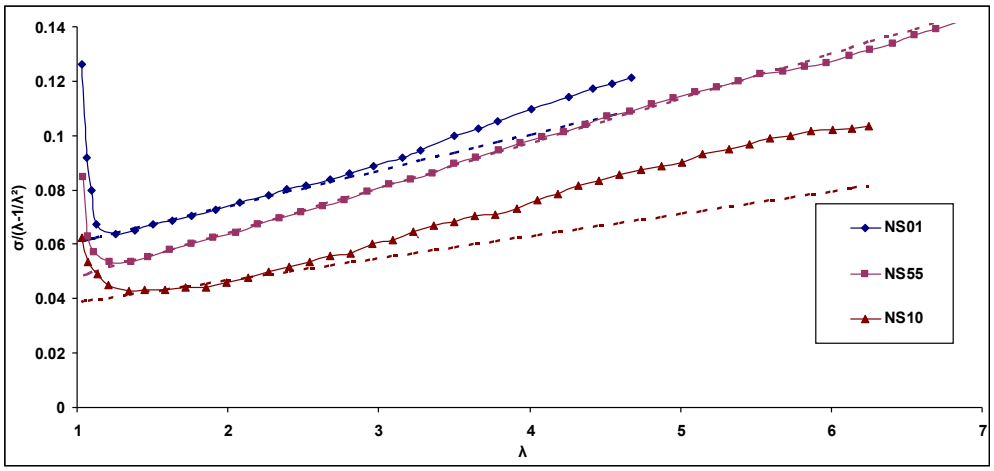


**Figure (8)** Relation between $\sigma\Big/\left(\lambda-\frac{1}{\lambda^2}\right)$ and $\lambda$ for three selected NS samples

Table 11. The constants $C_1$ and $C_2$ for NS samples

| | NS01 | NS19 | NS28 | NS37 | NS46 | NS55 | NS64 | NS73 | NS82 | NS91 | NS10 |
|---|---|---|---|---|---|---|---|---|---|---|---|
| $C_1$ ($\times 10^3$) | 13.13 | 13.63 | 14.4 | 15.2 | 15.94 | 16.45 | 15.51 | 13.04 | 11.05 | 9.27 | 8.17 |
| $C_2$ ($\times 10^3$) | 47.74 | 44.1 | 41.2 | 39 | 36.7 | 34.6 | 33.2 | 32.3 | 31.7 | 31.1 | 30.42 |
| $R^2$ | 0.976 | 0.881 | 0.986 | 0.97 | 0.991 | 0.997 | 0.992 | 0.986 | 0.96 | 0.89 | 0.878 |

Table 12. Power low, $R^2$ value and $f$ value for NS55N2 and NS55N7 samples

| Samples | NS55N2 | NS55N7 |
|---|---|---|
| Power low | $fC = 0.1040\times(\mathrm{N220\,phr})^{0.6413}$ | $fC = 0.0684\times(\mathrm{N774\,phr})^{0.7268}$ |
| $R^2$ | 0.999 | 0.996 |
| $f$ value | 6.99 | 6.37 |

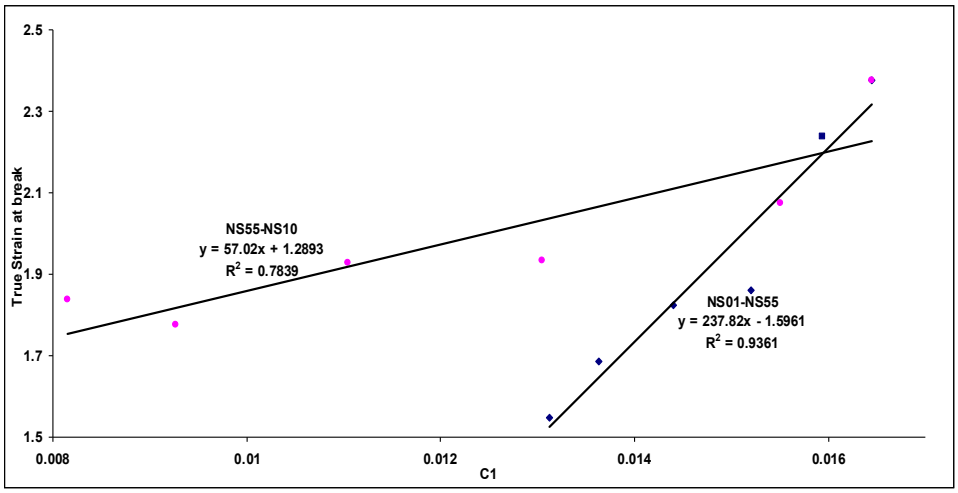


Figure 9. Constant $C_1$ versus true strain at break for NS samples

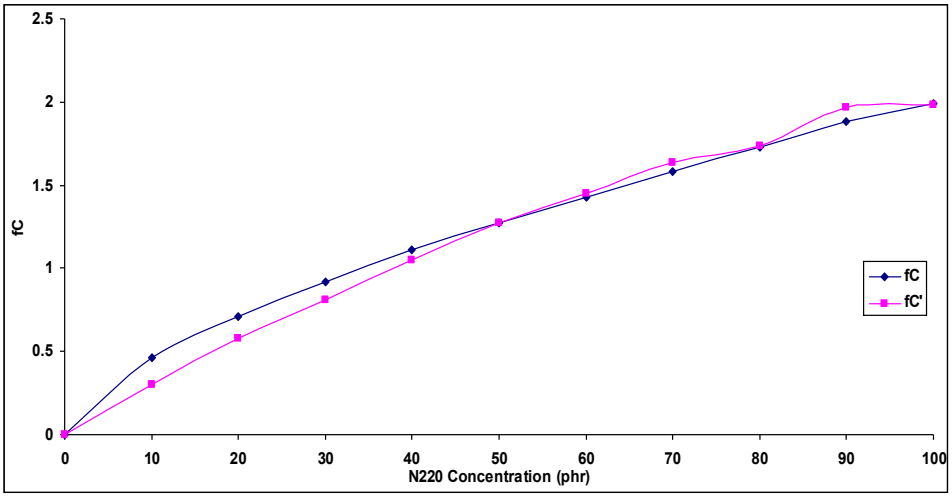


Figure 10. Factor *fC* versus N220 phr concentration for NS55N2 samples, the power low fitting is not shown in the graph

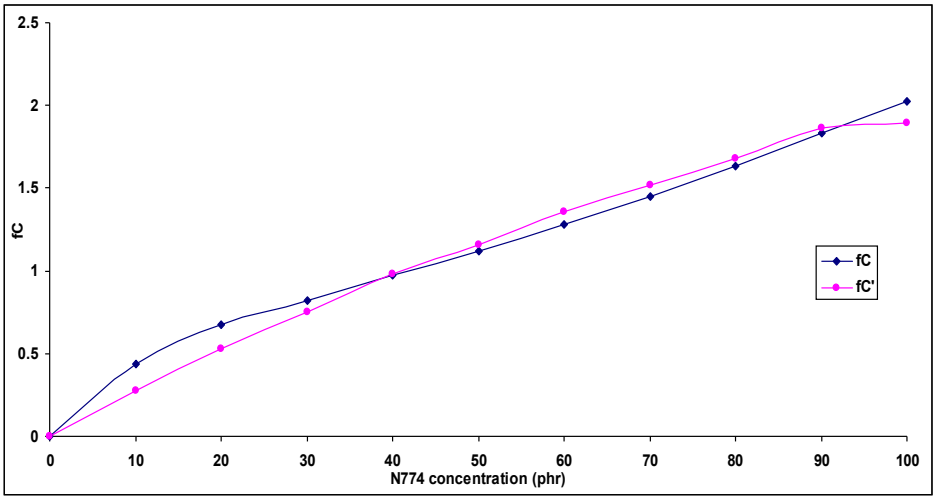


Figure 11. Factor *fC* versus N774 phr concentration for NS55N7 samples, the power low fitting is not shown in the graph

## 4. Conclusion

It may be concluded that, the NR/SBR blend exhibits optimum values of tensile strength and elongation at break can be achieved at equal ratios of rubbers (50NR/50SBR). The incorporation of this blend with carbon black N220 and N774 enhance the mechanical properties. N220 black carbon defines its own optimum at 40 phr while N774 carbon at 60 phr.

For mixed types of black, there is no remarkable effect for the order of addition on the values of tensile strength and/or elongation at break.

The theoretical model Mooney-Rivlin was applied to the NR/SBR blends and shows the maximum number of links appears for blend which has two equal ratios of rubbers in good agree to experimental data.

Guth, Simha and Gold filler volume concentration equation was applied to NS55N2 and NS55N7 samples and fitted to power low which relates the filler phr concentration to its volume concentration for carbon blacks N220 and N774.

**Corresponding Author:**
Dr. A.S. Abdel-Rahman
Physics Department
Faculty of Science
Cairo University, Giza, Egypt
E-mail: *asabry@sci.cu.educ.com

## References

1. H.N.M. Alsuhaiqi, A.A. El-Gamel, S.A. Khairy, and H.H. Hassan, Nat. Sci., 12(8), 154 (2014).
2. T.M. Nair, M.G. Kumaran, and G. Unnikrishnan, J. Appl. Polym. Sci., 93, 2606 (2004).
3. A.M.Y. El-Lawindy, Egypt. J. Sol., 25, 93 (2002).
4. L. Ji-Zhao, Polymer Testing, 24(4), 435 (2005).
5. Geyou, H. Quanli, and K. Myung-Soo, Carbon Letters, 9, 115 (2008).
6. P. Hajji, L. David, J.F. Gerard, J.P. Pascault, and G. Vigier, J. Polym. Sci. Polym. Phys., 37(22), 3172 (1999).
7. J.E. An, and Y.G. Jeong, Eur. Polym. J., 49(6), 1322 (2013).
8. X.W. Zhou, Y.F. Zhu, and J. Liang, Materials Research Bulletin, 42(3), 456 (2007).
9. F.T. Wall, J. Chem. Phys., 11, 527 (1943).
10. P.J. Flory, "Principle of Polymer Chemistry", Cornell University Press (1953).
11. H.M. James, and E. Guth, J. Chem. Phys., 11, 455 (1943).
12. M. Mooney, J. App. Phys., 11, 582 (1940).
13. R. S. Rivlin, Phil. Trans. Royal Soc. London, A240, 459 (1948).
14. E. Guth and R. Simha, Kolloid Z., 74, 266 (1936).
15. E. Guth, J. Appl. Phys., 16, 20 (1945).
16. ASTM D 3182 (2012).
17. ASTM D 412-80 (2013).
18. T. Proulx, Dynamic Behavior of Materials, Volume 1, Conference Proceedings of the Society for Experimental Mechanics Series, 1, 361 (2011).
19. H.S. Kaufman, and J.J. Falcetta, Introduction to Polymer Science and Technology, John Wiley and Sons, Inc., N Y, 330 (1977).
20. M.M. Hassan, A.A. Abd El-Megeed, and N.A. Maziad, Polymer Composites, 30(6), 743 (2009).
21. Gold, Thesis, Vienna (1937).

8/3/2015